Available online at www.sciencedirect.com
ScienceDirect
Journal of Sound and Vibration 300 (2007) 379–386
JOURNAL OF SOUND AND VIBRATION
www.elsevier.com/locate/jsvi

Short Communication

Vibration of multi-layered bands with interfacial imperfection

B. Kovács

Institute of Mathematics, University of Miskolc, Miskolc - Egyetemváros 3515, Hungary

Received 6 June 2005; received in revised form 13 December 2005; accepted 12 January 2006
Available online 13 November 2006

Abstract

A new laminate model is presented for the dynamic analysis of laminated band. The bond between any two adjacent layers is assumed either perfect or imperfect, which is uniformly described by a general spring-layer model. The differential equations which govern the free vibrations of a band and the associated boundary conditions are derived by Hamilton's principle considering bending, shear and normal deformation of all layers. The author used a new iterative process to successively refine the stress/strain field in the layers. The model includes the effects of transverse shear and rotatory inertia. The iterative model is used to predict the modal frequencies of simply supported laminated band. Numerical examples are finally considered and discussed.

1. Introduction

The predictor–corrector approach appears to have high potential for the accurate prediction of vibration frequencies, stresses, and deformations in multi-layered composite plates and shells. Accurate determination of the stress and displacement fields is particularly important for "stress critical" calculation such as delamination. Noor and Burton [1] presented a predictor–corrector approach for the analysis of composite plates. The authors used a plate model based on first-order shear deformation theory, coupled with integration of the equilibrium equations, to refine the estimate of the local stress field through the thickness of the laminate. The refined stress field was also used to generate improved estimates of the shear correction factors in the first-order shear deformation model, leading to improved estimates of the plate displacements and natural frequencies. Vijayakumar and Krishna Murty [2] developed a smeared laminate model for the static analysis of laminated plates that could, in fact, accurately predict the stress distribution in general laminates. Zapfe and Lesieutre [3] presented a variation of Vijayakumar and Krishna Murty's static method for laminated beams. Note that in these works, the interlaminar bonding is always assumed to be perfect. In practice, however, the bond may be weakened either in the process of manufacture because of the introduction of small flaws or during service when microcracks are induced under various conditions. There has been a number of works related to elastic laminated structures involving the effect of interlaminar bonding imperfections [4,5].

The present research extends the iterative smeared laminate model developed by Zapfe and Lesieutre to the dynamic analysis of laminated bands. The word band is used to denote a rectangular plate in the plane strain state. The bond between any two adjacent layers is assumed either perfect or imperfect, which is uniformly described by a general spring-layer model. Numerical examples are finally considered and discussed.

0022-460X/$ - see front matter © 2006 Published by Elsevier Ltd.
doi:10.1016/j.jsv.2006.01.018

2. Basic theory

Consider an n-layered medium as shown in Fig. 1. The z-axis is out-of-plane, with the x and y axes corresponding to the respective axial and transverse coordinates of the laminate. The $x-z$ plane coincides with the mid-plane of the band. The laminate is assumed to be infinitely long in the z-direction, with imperfect bonding between layers. We assume that its two edges are simply supported as described by the end conditions on the laminate. The quantities related to ith layer are suffixed by a subscript (i) while those related to ith interface are attached by a subscript $[i]$. The laminate is of length L, the total thickness is H, and the ith layer has thickness $h_{(i)}$. Layer 1 is the bottom layer of the laminate and layer n is the top layer. Layer i is bonded by the lower interface $y_{[i]}$ and the upper interface $y_{[i+1]}$ with thickness $h_{(i)} = y_{[i+1]} - y_{[i]}$; $y_{[i]}$ are signed distances of the interfaces from the mid-plane. It is obvious that $-H/2 = y_{[1]} < y_{[2]} < \cdots < y_{[i]} < y_{[i+1]} < \cdots < y_{[n]} < y_{[n+1]} = H/2$. The ith lamina occupies the domain defined by $y_{[i]} < y < y_{[i+1]}$, $i = 1, \ldots, n$ (Fig. 2).

Each of the n layers has the constitutive relations

$$\sigma_{11(i)} = C_{11(i)}\varepsilon_{11(i)} + C_{12(i)}\varepsilon_{22(i)}, \tag{1}$$

$$\sigma_{22(i)} = C_{12(i)}\varepsilon_{11(i)} + C_{22(i)}\varepsilon_{22(i)}, \tag{2}$$

$$\sigma_{33(i)} = C_{13(i)}\varepsilon_{11(i)} + C_{23(i)}\varepsilon_{22(i)}, \tag{3}$$

$$\sigma_{12(i)} = C_{66(i)}\varepsilon_{12(i)}, \tag{4}$$

where $\sigma_{11(i)}$, $\sigma_{22(i)}$, $\sigma_{33(i)}$ and $\sigma_{12(i)}$ are stresses, $\varepsilon_{11(i)}$, $\varepsilon_{22(i)}$ and $\varepsilon_{12(i)}$ strains, and $C_{11(i)}$, $C_{12(i)}$, $C_{13(i)}$, $C_{22(i)}$, $C_{23(i)}$ and $C_{66(i)}$ elastic stiffnesses.

In the present model, the layerwise displacement field is written in the general form as

$$\begin{aligned}\mathbf{t}_{(i)}(x, y, t) &= u_{(i)}(x, y, t)\mathbf{e}_x + v_{(i)}(x, y, t)\mathbf{e}_y \\ &= \left[u_0(x, t) - y\frac{\partial v_0}{\partial x} + f_{(i)}(y)u_1(x, t)\right]\mathbf{e}_x + [v_0(x, t) + g_{(i)}(y)v_1(x, t)]\mathbf{e}_y,\end{aligned} \tag{5}$$

where $u_0(x, t)$, $v_0(x, t)$ denote the axial and transverse displacement of a point $(x, 0)$ on the mid-plane of the band, respectively. The terms $f_{(i)}(y)u_1(x, t)$ and $g_{(i)}(y)v_1(x, t)$ can be thought to be correction to account for transverse shear and normal deformation effects, respectively. The functions $f_{(i)}(y)$ and $g_{(i)}(y)$ represent the shape of the corrections through the thickness of the band, while $u_1(x, t)$ and $v_1(x, t)$ determine its distribution along the length. The solution of a given problem requires the determination of the unknown functions, $u_0(x, t)$, $u_1(x, t)$, $v_0(x, t)$, $v_1(x, t)$, $f_{(i)}(y)$ and $g_{(i)}(y)$. By using the standard expressions

$$\mathbf{t} = u\mathbf{e}_x + v\mathbf{e}_y, \quad \varepsilon_{11} = \frac{\partial u}{\partial x}, \quad \varepsilon_{12} = \frac{\partial v}{\partial x} + \frac{\partial u}{\partial y}, \quad \varepsilon_{22} = \frac{\partial v}{\partial y},$$

the strain tensor of each layer can be computed from Eq. (5):

$$\varepsilon_{11(i)} = \frac{\partial u_0}{\partial x} - y\frac{\partial^2 v_0}{\partial x^2} + f_{(i)}(y)\frac{\partial u_1}{\partial x}, \tag{6}$$

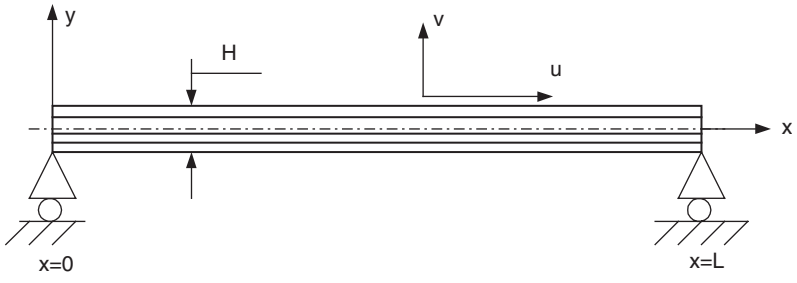

Fig. 1. Band configuration.

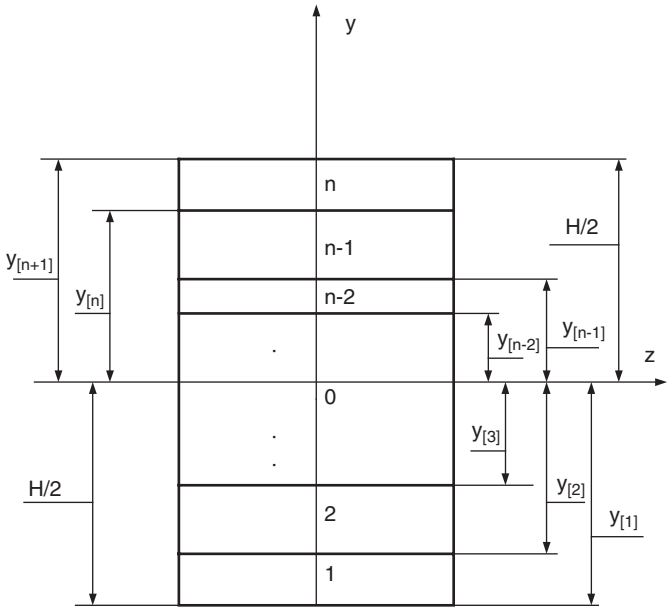

Fig. 2. Configuration and coordinate system of an n-layered medium.

$$\varepsilon_{12(i)} = \frac{\mathrm{d}f_{(i)}}{\mathrm{d}y} u_1(x,t) + g_{(i)}(y)\frac{\partial v_1}{\partial x}, \tag{7}$$

$$\varepsilon_{22(i)} = \frac{\mathrm{d}g_{(i)}}{\mathrm{d}y} v_1(x,t), \tag{8}$$

$$\varepsilon_{33(i)} = 0. \tag{9}$$

The strain energy stored in the band has components associated with extension, shear and transverse normal deformation and is given by

$$U = \frac{1}{2}\sum_{i=1}^{n}\int_{x=0}^{L}\int_{y_{[i]}}^{y_{[i+1]}} [\sigma_{11(i)}\varepsilon_{11(i)} + \sigma_{22(i)}\varepsilon_{22(i)} + \sigma_{12(i)}\varepsilon_{12(i)}]\,\mathrm{d}x\,\mathrm{d}y. \tag{10}$$

The kinetic energy, which includes components associated with transverse, in-plane and rotary inertia, is given by

$$T = \frac{1}{2}\sum_{i=1}^{n}\int_{x=0}^{L}\int_{y_{[i]}}^{y_{[i+1]}} \rho_{(i)}\left(\frac{\partial \mathbf{t}_{(i)}}{\partial t}\right)^2 \mathrm{d}x\,\mathrm{d}y. \tag{11}$$

3. General spring-layer model

At an arbitrary interface, say the one between the $i-1$th layer and ith layer ($y = y_{[i]}$), we adopt the following general spring-layer model to describe the interfacial imperfection:

$$\sigma_{22(i)}(x, y_{[i]}) = \sigma_{22(i-1)}(x, y_{[i]}) = (v_{(i)}(x, y_{[i]}) - v_{(i-1)}(x, y_{[i]}))/R_{y[i]}, \tag{12}$$

$$\sigma_{12(i)}(x, y_{[i]}) = \sigma_{12(i-1)}(x, y_{[i]}) = (u_{(i)}(x, y_{[i]}) - u_{(i-1)}(x, y_{[i]}))/R_{x[i]}, \tag{13}$$

where $R_{y[i]}$ and $R_{x[i]}$ are the compliance coefficients of the model. For further discussion, the reader is referred to Ref. [4]. Eqs. (12) and (13) now take the following form as a result of the substitution of Eq. (5):

$$\sigma_{22(i)}(x, y_{[i]}) = \sigma_{22(i-1)}(x, y_{[i]}) = (g_{(i)}(y_{[i]}) - g_{(i-1)}(y_{[i]}))v_1/R_{y[i]} = \Delta g_{[i]} v_1/R_{y[i]}, \tag{14}$$

$$\sigma_{12(i)}(x, y_{[i]}) = \sigma_{12(i-1)}(x, y_{[i]}) = (f_{(i)}(y_{[i]}) - f_{(i-1)}(y_{[i]}))u_1/R_{x[i]} = \Delta f_{[i]} u_1/R_{x[i]}. \tag{15}$$

In the present study, imperfections opening in tension are not considered to avoid the material penetration phenomenon [4]. Under these considerations, the work due to the interfacial shear slip is given by

$$W = \frac{1}{2}\int_{x=0}^{L}\sum_{i=1}^{n-1}\sigma_{12(i)}(x, y_{[i]})\Delta u_{[i]}\,\mathrm{d}x = \frac{1}{2}\int_{x=0}^{L}\sum_{i=1}^{n-1}(\Delta f_{[i]})^2(u_1)^2/R_{x[i]}\,\mathrm{d}x. \tag{16}$$

4. Dynamic simply supported beams

The differential equations of motion and boundary conditions are derived using Hamilton's principle. The equations of motion for the four unknown functions, $v_0(x,t)$, $v_1(x,t)$, $u_0(x,t)$ and $u_1(x,t)$ are:

$$K_1\frac{\partial^2 u_0}{\partial x^2} - K_4\frac{\partial^3 v_0}{\partial x^3} + K_5\frac{\partial^2 u_1}{\partial x^2} + K_7\frac{\partial v_1}{\partial x} - M_1\frac{\partial^2 u_0}{\partial t^2} + M_4\frac{\partial^3 v_0}{\partial x\partial t^2} - M_5\frac{\partial^2 u_1}{\partial t^2} = 0, \tag{17}$$

$$\left(K_{11} + \sum_{i=1}^{n-1}(\Delta f_{[i]})^2/R_{x[i]}\right)u_1 + K_{12}\frac{\partial v_1}{\partial x} - K_3\frac{\partial^2 u_1}{\partial x^2} - K_5\frac{\partial^2 u_0}{\partial x^2} + K_6\frac{\partial^3 v_0}{\partial x^3} - K_9\frac{\partial v_1}{\partial x} + M_3\frac{\partial^2 u_1}{\partial t^2} + M_5\frac{\partial^2 u_0}{\partial t^2} - M_6\frac{\partial^3 v_0}{\partial x\partial t^2} = 0, \tag{18}$$

$$K_7\frac{\partial u_0}{\partial x} - K_8\frac{\partial^2 v_0}{\partial x^2} + (K_9 - K_{12})\frac{\partial u_1}{\partial x} + K_{10}v_1 - K_{13}\frac{\partial^2 v_1}{\partial x^2} + M_7\frac{\partial^2 v_0}{\partial t^2} + M_8\frac{\partial^2 v_1}{\partial t^2} = 0, \tag{19}$$

$$K_2\frac{\partial^4 v_0}{\partial x^4} - K_4\frac{\partial^3 u_0}{\partial x^3} - K_6\frac{\partial^3 u_1}{\partial x^3} - K_2\frac{\partial^2 v_0}{\partial x^2} - M_2\frac{\partial^4 v_0}{\partial x^2\partial t^2} + M_4\frac{\partial^3 u_0}{\partial x\partial t^2} + M_6\frac{\partial^3 u_1}{\partial x\partial t^2} + M_1\frac{\partial^2 v_0}{\partial t^2} + M_7\frac{\partial^2 v_1}{\partial t^2} = 0 \tag{20}$$

and the simply supported boundary conditions, specified at $x = 0$ and L, are given by

$$K_1\frac{\partial u_0}{\partial x} + K_4\frac{\partial u_1}{\partial x} + K_1 v_1 = 0, \tag{21}$$

$$K_4\frac{\partial u_0}{\partial x} - K_5\frac{\partial^2 v_0}{\partial x^2} + K_3\frac{\partial u_1}{\partial x} + K_9 v_1 = 0, \tag{22}$$

$$K_2\frac{\partial^2 v_0}{\partial x^2} - K_5\frac{\partial u_1}{\partial x} - K_8 v_1 = 0, \tag{23}$$

$$v_0 = v_1 = 0. \tag{24}$$

K_{1-13} and M_{1-8} are section stiffness and mass coefficients, given by

$$K_{[1,\ldots,6]} = \sum_{i=1}^{n}\int_{y_{[i]}}^{y_{[i+1]}} C_{11(i)}[1,\ y^2,\ f_{(i)}^2(y), y,\ f_{(i)}(y),\ yf_{(i)}(y)]\,\mathrm{d}y, \tag{25}$$

$$K_{[7,8,9]} = \sum_{i=1}^{n}\int_{y_{[i]}}^{y_{[i+1]}} C_{12(i)}\left[\frac{\mathrm{d}g_{(i)}}{\mathrm{d}y}, y\frac{\mathrm{d}g_{(i)}}{\mathrm{d}y}, f_{(i)}(y)\frac{\mathrm{d}g_{(i)}}{\mathrm{d}y}\right]\mathrm{d}y, \tag{26}$$

$$K_{[10]} = \sum_{i=1}^{n}\int_{y_{[i]}}^{y_{[i+1]}} C_{22(i)}\left(\frac{\mathrm{d}g_{(i)}}{\mathrm{d}y}\right)^2\mathrm{d}y, \tag{27}$$

$$K_{[11,12,13]} = \sum_{i=1}^{n}\int_{y_{[i]}}^{y_{[i+1]}} C_{66(i)}\left[\frac{\mathrm{d}g_{(i)}}{\mathrm{d}y}, y\frac{\mathrm{d}g_{(i)}}{\mathrm{d}y}, f_{(i)}(y)\frac{\mathrm{d}g_{(i)}}{\mathrm{d}y}\right]\mathrm{d}y, \tag{28}$$

$$M_{[1,\ldots,8]} = \sum_{i=1}^{n} \int_{y_{[i]}}^{y_{[i+1]}} \rho_{(i)}[1, y^2, f_{(i)}^2(y), y, f_{(i)}(y), yf_{(i)}(y), g_{(i)}(y), g_{(i)}^2(y)]\,\mathrm{d}y. \tag{29}$$

In the present formulation, the integrals are evaluated numerically using a trapezoidal method.

Functions that satisfy the differential equations and boundary conditions are:

$$v_0(x,t) = V_0 \sin(k_n x)\mathrm{e}^{\mathrm{i}\omega_n t}, \tag{30}$$

$$v_1(x,t) = V_1 \sin(k_n x)\mathrm{e}^{\mathrm{i}\omega_n t}, \tag{31}$$

$$u_0(x,t) = U_0 \cos(k_n x)\mathrm{e}^{\mathrm{i}\omega_n t}, \tag{32}$$

$$u_1(x,t) = U_1 \cos(k_n x)\mathrm{e}^{\mathrm{i}\omega_n t}, \tag{33}$$

where $k_n = (n\pi)/L$. Substitution of Eqs. (30)–(33) into Eqs. (17)–(20) leads to a matrix equation for the coefficients (V_0, V_1, U_0, U_1):

$$[-\omega_n^2[M] + [Y]]\{U\} = 0, \quad \{U\} = \{V_0, V_1, U_0, U_1\}, \tag{34}$$

$$Y = \begin{bmatrix} k_n^4 K_4 & k_n^2 K_8 & -k_n^3 K_4 & -k_n^3 K_6 \\ k_n^2 K_8 & K_{10} + k_n^2 K_{13} & -k_n K_7 & k_n K_{12} - k_n K_9 \\ -k_n^3 K_4 & -k_n K_7 & k_n^2 K_1 & k_n^2 K_5 \\ -k_n^3 K_6 & k_n K_{12} - k_n K_9 & k_n^2 K_5 & K_{11} + \sum_{i=1}^{n-1} (\Delta f_{[i]})^2 / R_{x[i]} + k_n^2 K_3 \end{bmatrix},$$

$$M = \begin{bmatrix} M_1 + k_n^2 M_2 & M_7 & -k_n M_4 & -k_n M_6 \\ M_7 & M_8 & 0 & 0 \\ -k_n M_4 & 0 & M_4 & M_5 \\ -k_n M_6 & 0 & M_5 & M_3 \end{bmatrix}.$$

The eigensolution yields four frequencies and mode shapes for each wavenumber.

5. Improved estimate for correction functions

The equations of motion, $\sigma_{kl,k} = \rho \partial^2 u_l / \partial t^2$, applied to the ith layer of the band are now in the form

$$\frac{\partial \sigma_{11(i)}}{\partial x} + \frac{\partial \sigma_{12(i)}}{\partial y} = \rho_{(i)} \frac{\partial^2 u_{(i)}}{\partial t^2}, \tag{35}$$

$$\frac{\partial \sigma_{12(i)}}{\partial x} + \frac{\partial \sigma_{22(i)}}{\partial y} = \rho_{(i)} \frac{\partial^2 v_{(i)}}{\partial t^2}. \tag{36}$$

In the predictor phase, the linear or cubic zig-zag model is used to provide the initial estimate of $u_{(i)}$ and $v_{(i)}$ from which the in-plane stresses $\sigma_{11(i)}$ can be found. Using the results from one of the two models, the transverse shear and normal stress are calculated by integrating the three-dimensional equilibrium equations (35)–(36) in the thickness direction. In the plane strain state, these are:

$$\sigma_{12(i)} = \int_{y_{[i]}}^{y} \rho_{(i)} \frac{\partial^2 u_{(i)}}{\partial t^2} - \frac{\partial \sigma_{11(i)}}{\partial x}\,\mathrm{d}y, \tag{37}$$

$$\sigma_{22(i)} = \int_{y_{[i]}}^{y} \rho_{(i)} \frac{\partial^2 v_{(i)}}{\partial t^2} - \frac{\partial \sigma_{12(i)}}{\partial x}\,\mathrm{d}y. \tag{38}$$

In the corrector phase, the transverse shear and the normal stress distribution found earlier are used to determine the new corrector functions $f_{(i)}(y)$ and $g_{(i)}(y)$ in the layerwised displacement field.

Substitution of Eqs. (6)–(8) and (30)–(33) in Eqs. (2) and (4) yield the following set of differential equations in terms of the new correction functions $f_{(i)}(y)$ and $g_{(i)}(y)$:

$$C_{11(i)}V_1\frac{\mathrm{d}g_{(i)}}{\mathrm{d}y} - C_{12(i)}k_nU_1f_{(i)}(y) = \sigma_{22(i)} - C_{12(i)}(-U_0k_n + yk_n^2V_0), \tag{39}$$

$$C_{66(i)}U_1\frac{\mathrm{d}f_{(i)}}{\mathrm{d}y} + C_{66(i)}V_1k_ng_{(i)}(y) = \sigma_{12(i)}. \tag{40}$$

The effect of interfacial bonding imperfections can be easily taken into account in the solution of Eqs. (39)–(40) by using Eq. (15).

6. Results and discussion

Two examples are considered in this section: a three-layer laminate of dissimilar elastic materials and a five-layer configuration. All laminates are composed of materials termed A and B. Detailed material properties are listed in Table 1. In all examples to be considered, we take $R_{x[i]} = HR/C_{66(1)}$ for simplicity. The bonding imperfections will be measured in terms of the dimensionless sliding parameter R.

Three-layer laminate ($A/B/A$): Two layers of material A are bonded to the top and bottom of the elastic material B. The thicknesses of the A layers are 4 and 5 mm with the total laminate thickness 13 mm.

Five-layer laminate ($A/B/A/B/A$): In order to demonstrate a multi-ply example, the three-layer laminate was modified such that the shear core was split into two equal thickness (2 mm) layers. The core layers were interspersed among three equal thickness (3 mm) layers of the facesheet material A.

In the examples presented below, the span-to-thickness ratios L/H are equal to 5, 10 and 50. For the first natural frequencies ($n = 1$), representative through-thickness distributions of the elastic field variables are shown for the three-layer laminate. These have been normalized by dividing through by the maximum value for each field variable. The through-thickness distributions for transverse shear stress $\sigma_{12(i)}$ and transverse normal stress $\sigma_{22(i)}$, are shown in Figs. 3 and 4. These figures are associated with perfect bonding between layers ($R = 0$). The resulting frequencies are shown in Table 2. Results are given in terms of natural frequencies in hertz. Fig. 3 shows the transverse shear stress distribution for length to thickness ratios of $L/H = 50$ and $L/H = 5$. In this figure, the solid line corresponds to the case $L/H = 50$, with the dashed line used for $L/H = 5$. The shear stress is about constant in the core because the shear gradient, from Eq. (35) is effectively zero. Fig. 4 shows the normal stress distribution for the three layer band with length-to-thickness ratio of $L/H = 50$. As expected, the behavior is approximately symmetric about the mid-line for this geometry. Table 2 shows the effect of the interfacial imperfections on the first natural frequencies for the three-layer laminate and the five-layer configuration. The span-to-thickness ratios L/H are equal to 5, 10 and 50 and the imperfections of the two interfaces are identical, i.e. $R_{x[i]} = HR/C_{66(1)}$. It can be shown that the results for the perfect laminate ($R = 0$) agree well with those obtained by Zapfe and Lesieutre [3]. Thus, the correctness of algebra as well as program of our method is verified. The interfacial imperfections will lower the natural frequency because of the reduction of overall stiffness of the laminate. Table 3 shows the effect of the interfacial imperfections on the second natural frequencies for the three-layer laminate and the five-layer configuration. Fig. 5 depict the eigenfrequency ratio, i.e., the ratio between the eigenfrequency corresponding

Table 1
Elastic properties of materials

Property	A	B
C_{11} (GPa)	8.13	1.075
C_{12}	0.0433	0.0032
C_{22}	6.45	0.75
C_{33}	2.6	0.36
ρ (kg/m^3)	2.7	1.5

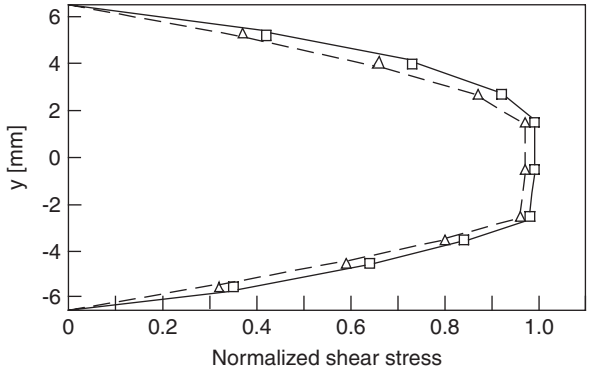

Fig. 3. Transverse shear stress distribution for three layer example: $L/H = 50$.

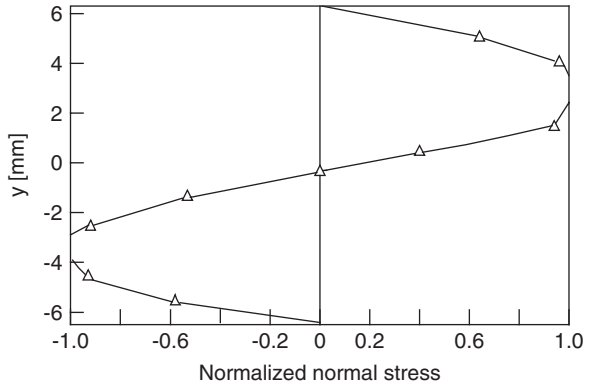

Fig. 4. Transverse normal stress distribution for three layer example: $L/H = 50$.

Table 2
Variation of the first natural frequency [Hz] with the compliance coefficient

H/L	[3] $R = 0$	Present theory		
		$R = 0$	$R = 0.1$	$R = 0.2$
$A/B/A$				
50	8.087×10	8.087×10	8.084×10	8.081×10
10	1.9069×10^3	1.9069×10^3	1.8893×10^3	1.870×10^3
5	6.618×10^3	6.618×10^3	6.383×10^3	6.09×10^3
$A/B/A/B/A$				
50	7.692×10	7.692×10	7.687×10	7.683×10
10	1.836×10^3	1.836×10^3	1.814×10^3	1.793×10^3
5	6.528×10^3	6.528×10^3	6.06×10^3	5.604×10^3

to the value of R considered and that corresponding to $R = 0$, as a function of the length to thickness ratio, for selected imperfections R. The interfacial parameter has the values $R = 0, 0.2, 0.4, 0.6$. These values represent a decreasingly stiff interphase, i.e. a progressively weakened bonding, with $R = 0$ corresponding to a perfect bond. Therefore, increasing R means relaxation of the interfacial bonding strength, and hence reduction in the overall rigidity of bands. Thus, as expected, increasing the parameter R causes reductions in interface stresses

Table 3
Variation of the second natural frequency [Hz] with the compliance coefficient

H/L	[3] $R=0$	Present theory		
		$R=0$	$R=0.1$	$R=0.2$
$A/B/A$				
50	3.21×10^{2}	3.21×10^{2}	3.204×10^{2}	3.199×10^{2}
10	6.619×10^{3}	6.619×10^{3}	6.3786×10^{3}	6.1206×10^{3}
5	1.936×10^{4}	1.936×10^{4}	1.897×10^{4}	1.862×10^{4}
$A/B/A/B/A$				
50	3.058×10^{2}	3.058×10^{2}	3.051×10^{2}	3.042×10^{2}
10	6.528×10^{3}	6.528×10^{3}	6.114×10^{3}	5.614×10^{3}
5	1.953×10^{4}	1.953×10^{4}	1.88×10^{4}	1.815×10^{4}

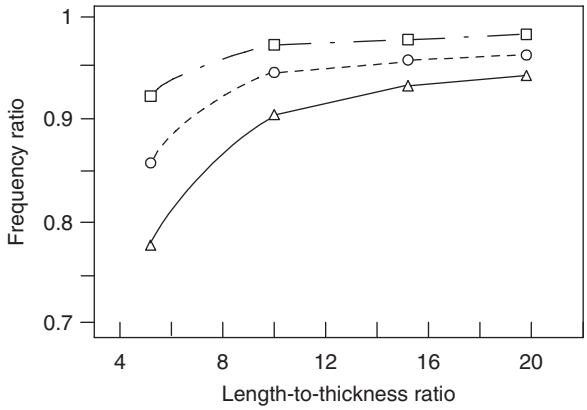

Fig. 5. Frequency ratio for three layer example: $R=0.6$; $R=0.4$; $R=0.2$.

which are beneficial, but at the expense of increases of the central deflection. A smeared laminate model has been presented that can accurately determine the dynamic stress distribution in general laminated bands. Accurate determination of the stress and displacement fields is particularly important for ''stress critical'' calculation such as delamination.

References

[1] A.K. Noor, W.S. Burton, Stress and free vibration analyses of multilayered composite plates, *Computers and Structures* 11 (1989) 183–204.
[2] K. Vijayakumar, A.V. Krishna Murty, Iterative modeling for stress analysis of composite laminates, *Composite Science and Technology* 32 (1995) 165–181.
[3] J.A. Zapfe, G.A. Lesieutre, Vibration analysis of laminated beams using an iterative smeared laminate model, *Journal of Sound and Vibration* 199 (1997) 275–284.
[4] Z.Q. Cheng, A.K. Jemah, F.W. Williams, Theory for multilayered anisotropic plates with weakened interfaces, *Journal of Applied Mechanics* 63 (1996) 1019–1026.
[5] U. Icardi, Free vibration of composite beams featuring interlaminate bonding imperfections and exposed to thermomechanical loading, *Composite Structures* 46 (1999) 229–243.